BNL 29923
OG 598
CONF-810615--1

FINE-GRAINED HODOSCOPES BASED ON SCINTILLATING OPTICAL FIBERS

S.R. Borenstein, York College, CUNY
New York, NY

R.C. Strand, BNL
Upton, NY

MASTER

Talk presented at the

CESRII Workshop
Cornell University, Ithaca, NY
June 18, 1981

FINE GRAINED HODOSCOPES BASED ON SCINTILLATING OPTICAL FIBERS

S.R. Borenstein, York College, CUNY

and

R.C. Strand, BNL

Abstract

In order to exploit the high event rates at ISABELLE, it will be necessary to have fast detection with fine spatial resolution. The authors are currently constructing a prototype fine-grained hodoscope, the elements of which are scintillating optical fibers. The fibers have been drawn from commercially available plastic scintillator which has been clad with a thin layer of silicone. So far it has been demonstrated with one mm diameter fibers, that with a photodetector at each end, the fibers are more than 99% efficient for lengths of about 60 cm. The readout will be accomplished either with small diameter photomultiplier tubes or avalanche photodiodes used either in the linear or Geiger mode. The program of fiber development and evaluation will be described. The status of the APD as a readout element will be discussed. Finally, an optical encoding readout scheme will be described for events of low multiplicity.

Introduction

During the 1978 summer study[1] it was decided that a research and development program should be undertaken to develop a fine grained scintillating hodoscope to cope with the high rates expected. Early attempts[2] to produce long bare scintillating filaments of one mm diameter yielded maximum useful lengths of about 15 cm, presumably due to cumulative losses at the scintillator to air interface.[3] In order to increase the useful length of the scintillating fiber, the experience and expertise of the fiber optics industry was used to draw a fiber from a heated preform of polished PVT scintillator, and to coat this with a cladding of lower refractive index. The principle is illustrated in Figure 1 where those rays of light making an angle, relative to the fiber axis, of less than the numerical aperture angle

of the fiber are trapped and guided to the end of the fiber where they are detected by a photodetector. A desirable candidate for the photodetector is the avalanche photodiode (APD) which has the virtue of small size and immunity from magnetic fields. It has a photon to electron quantum efficiency about 4 times greater than that of a photomultiplier tube; however, the probability that the photoelectron will propagate to a usable signal is correspondingly lower. Thus the sensitivity of the APD is comparable to that of the PMT.

I. HODOSCOPE DESCRIPTION

A section of a hodoscope constructed from such scintillating fibers is shown schematically as a bilayer of fibers imbedded in a protective isolating matrix. The centers of the fibers are offset by one radius from one layer to the next to assure that there are no cracks through which a particle might pass without penetrating a reasonable depth of scintillator.

II. FIBER EVALUATION PROCEDURE

Experimental Setup

In order to establish the feasibility of such a hodoscope, Brookhaven National Laboratory entered into a contract with Galileo Electro-Optical Corporation[4] to undertake an experimental program to draw and clad scintillating fibers. Various commercially available scintillators, several cladding materials, curing methods, temperatures, tensions, and draw speeds were tried. The scintillators NE102, NE110 and NE161, were obtained from Nuclear Enterprises. The cladding materials have been a proprietary ultraviolet cured acrylic and a heat cured silicone. The best results to date have been obtained with silicone coated NE161. The layout of the test facility[5] appears in Figure 2. An electron from Ruthenium 106 penetrates two small telescope counters T_1 and T_2 which sandwhich the fiber. Upon a coincidence from T_1T_2, the signal from S1 is detected by an RCA 8850 photomultiplier with single photoelectron resolution. From the resultant spectrum in Figure 2 we can calculate the mean number of photoelectrons (4 in the example shown).

A crucial feature of the test equipment is the use of a PMT with single photoelectron resolution. In this way all light yield and attenuation data

are obtained in terms of absolute number of photoelectrons. The distance from the pedestal to the first peak sets the scale in absolute photoelectrons regardless of the gain of the PMT and the associated electronics. In principle, the light yield for a given spectrum is obtained by determining the mean of the distribution. In practice, for low light levels it is found empirically that the light yield is more easily determined by measuring the ratio of the heights of the second, third and fourth peaks. For higher light levels the mean is almost the same as the peak of the distribution.

Test Results

The highlights of the results obtained so far are shown in the curves of Figure 3 and in the accompanying table where each fiber is characterized by an attenuation length and an effective photoelectron yield at the origin. The data were obtained from fibers whose diameter varied from .032" to .090" but the results have all been scaled to a diameter of .054" or 1.37 mm. The progression of curves 1 through 3 show a steady improvement due in part to choice of material, and in part to gradually improved technique. Curve No. 4 underscores the drastic attenuation suffered at the scintillator to air surface. By using coincidence techniques and setting discriminator thresholds below the single photoelectron level it is possible to construct hodoscope elements from fibers of about 1 mm diameter in lengths approaching 1 meter.

III. READOUT OPTIONS

Individual Fiber Readout

A useful hodoscope will ultimately consist of hundreds of such scintillating fibers and we must now address ourselves to the problem posed by the readout of so many channels.

Two types of photodetectors have been considered for the readout elements. PMT's and APD's. In the former case, the necessary technology is at hand and the solution consists of devising a scheme to couple the many fibers individually to small diameter, highly sensitive photomultipliers.

The disadvantages of this solution are:

1. The bulkiness of PMT's relative to the fiber diameter.
2. The cost of the PMT's which probably will not come down in the near future.
3. The inability of PMT's to function in magnetic fields.

In the case of the APD, the size of the device is well matched to the size of the fiber, and the device itelf is unaffected by magnetic fields. The cost is comparable to that of a PMT, but as seems to be the case with all silicon, one can anticipate drastic cost reduction as these devices start to be produced in much larger quantities.

The main disadvantage of this solution is that one is dealing with a new technology, and there is no experience to indicate that the device can be successfully operated in the Geiger or saturated mode. In theory, with the APD cooled to about -70°C and biased above the breakdown voltage, a photoelectron has a small (on the order of 20%) probability of causing a breakdown signal. This propbability is an increasing function of the overvoltage, but the signal size is independent of the number of photoelectrons that contributed to it so that the signal contains no analog information, and it occurs with a probability which depends upon the overvoltage as well as the number of photoelectrons. On the other hand, there is a dynamic dark count proportional to the true counting rate, which also increases with overvoltage. Thus, there is an optimum overvoltage obtained by trading off required photoelectron input versus acceptable dark count as shown in Figure 4 which shows required photoelectron input versus overvoltage for a detection efficiency of 99.9%. The other curve shows the total to input counting ratio as a function of the overvoltage, thus for an acceptable dynamic dark count of 20% the required input is 22 photoelectrons per pulse.

Referring back to Figure 3, for fibers of about 1 mm diameter and 50 cm length, the number of photoelectrons expected with perfect optical coupling between fiber and APD is about 30. (8 from Figure 3 multiplied by 4 for the higher quantum efficiency of the APD). Unfortunately the coupling between fiber and APD is far from perfect, and a means of packaging the APD silicon chip to optimize the light coupling is yet to be developed.

Optically Encoded Readout

Under most circumstances, the high event rates and large multiplicities for which the fiber hodoscope is being developed would preclude any multiplexing schemes to reduce the number of readout channels. However for specific applications of low multiplicity it might be possible to effect considerable economies in readout electronics by the use of optical encoding.

Let us consider one layer of the hodoscope which contains n elements. At the upper end, the fibers are grouped in $\sqrt{n}$ bundles, each consisting of $\sqrt{n}$ neighboring fibers. At the lower end the fibers are also grouped in $\sqrt{n}$ bundles, but the groupings are such that the first bundle consists of the first fiber of each bundle at the upper end, the second bundle consists of the second fiber of each bundle at the upper end and so on. Thus a single fiber could be specified by a signal from one bundle at each end of the hodoscope. The number of readout channels has now been reduced from n to $2\sqrt{n}$. The problem with this scheme is that if more than one fiber is hit, the encoding is ambiguous. The level of ambiguity can be drastically reduced, by making use of the second layer of the hodoscope and arranging the bundles in groupings which are distinct from those already used. In practice this scheme is of interest when the number of elements is very large; for example 900 elements can be read out with just 60 photodetectors. However, for purposes of illustration we will describe a 2 x 25 element bilayer, as shown in Figure 5.

In this example, the simplest grouping is the ALPHA grouping, A,B,C,D,E each containing 5 successive fibers, at the lower end of the front layer. At the upper end of the front layer the first of each group of 5 goes to number 1 of the numerically grouped photodetectors. So far, a hit in the 9th fiber would give the signal B4. The rear layer is grouped as indicated by Greek letters at the upper end, and by Hebrew letters at the lower end. The four groupings can now be referred to as ALPHA, NUMERIC, GREEK and HEBREW. The same hit would now be characterized as B4εℵ.

In the examples shown, 3 hits in fibers, 2,9,20 would give rise to a 6-fold ambiguity if only one layer were available. The resolution of this amgiguity is illustrated by listing the expected signals for each ambiguous hypothesis as well as the number of absent signals and the number of extra signals for each hypothesis.

It is worth noting that with ALPHA and NUMERIC signals, the ambiguity is 6-fold, the addition of GREEK eliminates 4 of the ambiguities, and the final ambiguity is resolved only with the inclusion of the HEBREW group.

We also note that the ALPHA group can be used by itself as a hodoscope which is 5 times ($\sqrt{n}$) as coarse as the physical hodoscope.

Conclusion

So far we have demonstrated the feasibility of the scintillating fiber as a hodoscope element. To date the best results have been obtained with NE161 as the scintillating core and silicone as the cladding material. This combination is rather fragile and subject to deterioration with handling. To this end we are considering the application of a buffer coat, to protect the silicone cladding.

In addition we are studying several alternate cladding materials.

With regard to the optical readout, the preferred detector is the APD, and we are actively pursuing methods of both increasing the intrinsic sensitivity of the device, and improving the optical coupling between the fiber and the solid state chip.

This research was supported by the U.S. Department of Energy under contracts No. DE-AC02-76CH00016 and DE-AC02-81ER40035.

References

1. J. Marx and S. Ozaki, Topic I: Detectors and Experiments, Summary of Activity, Proc. 1977 ISABELLE Summer Workshop, BNL 50721, p. 4.
2. G.T. Reynolds and P.E. Condon, Rev. Sci. Instr. 28, No. 12, Dec. 1957; G.T. Reynolds, Nucleonics 16, No. 6, June 1958.
3. L. Reiffel and N.S. Kapany, Rev. Sci. Instr. 31, 1136-1142 (1960).
4. BNL Contract #463787-S with Galileo Electro-Optical Company.
5. S.R. Borenstein, R.B. Palmer and R.C. Strand, Optical Fibers and Avalanche Photodiodes for Scintillator Counters, presented at the International Conference on Experimentation at LEP, Uppsala, Sweden, 16-20 June, 1980: Physica Scripta, 23, No. 4:1, pp. 550-555 (April 1981) Ed: Tord Ekelof, Vol. 1-Invited Papers; Pub: Alden Press, Great Britain.

FIGURE CAPTIONS

Figure 1a. Sciltillating optical fiber, principle of operation;

b. Bilayer of fibers, encapsulated in isolating matrix.

Figure 2a. Fiber measurement setup: electron from source penetrates scintillators T_1 and T_2 as well as the fiber whose output signal S1 is analyzed;

b. Charge spectrum of fiber pulse using RCA 8850.

Figure 3. Attenuation curves for various fibers.

Figure 4. APD operation as a function of overvoltage.

Figure 5. Optical encoding and ambiguity resolution.

A schematic rendition of a 2 x 25 element bilayer ribbon. For ease of illustration, the fibers are drawn with a square cross section and the half-diameter shift from one layer to the next is not shown.

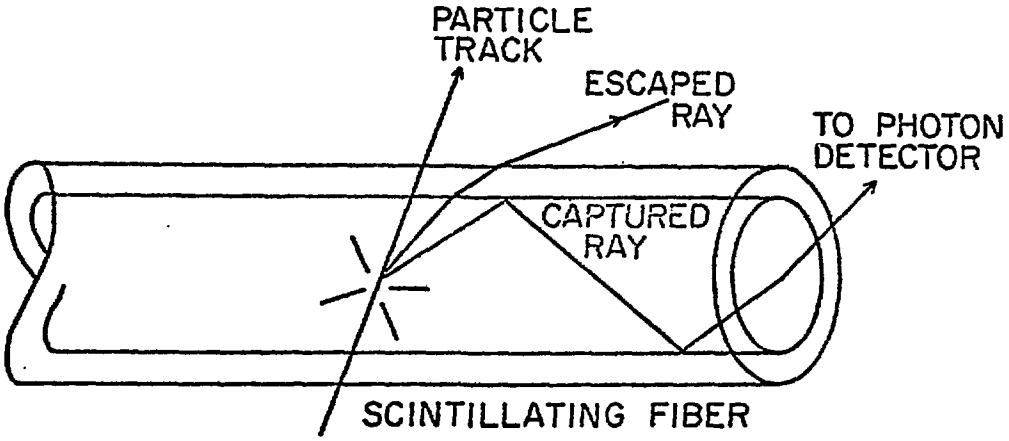

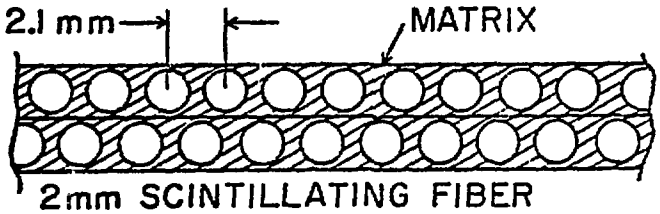

HODOSCOPE BILAYER

CHARGE SPECTRA OF SCINTILLATING FIBER USING RCA 8850 PHOTOMULTIPLIER

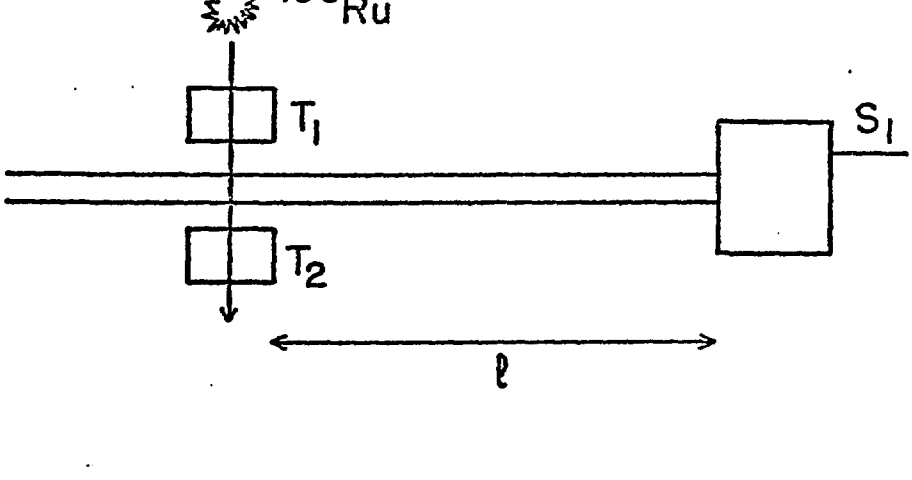

<n> ~ 4

SCINTILLATING FIBERS

FIBER COMPARISON SUMMARY
ALL RESULTS NORMALIZED TO $\phi = 0.054"$

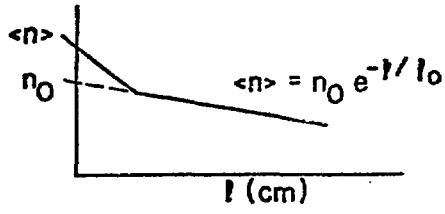

FIBER	ACTUAL ϕ	n_0	l_0	<n> AT l = 60
(1) NE110, UV-CLAD	0.054	6.3	85	3.1
(2) NE110, Si-CLAD	0.032	10.0	87	5.1
(3) NE161 Si-CLAD	0.090	13.5	200	10.0
(4) NE161 UNCLAD	0.032	6.8	65	<3

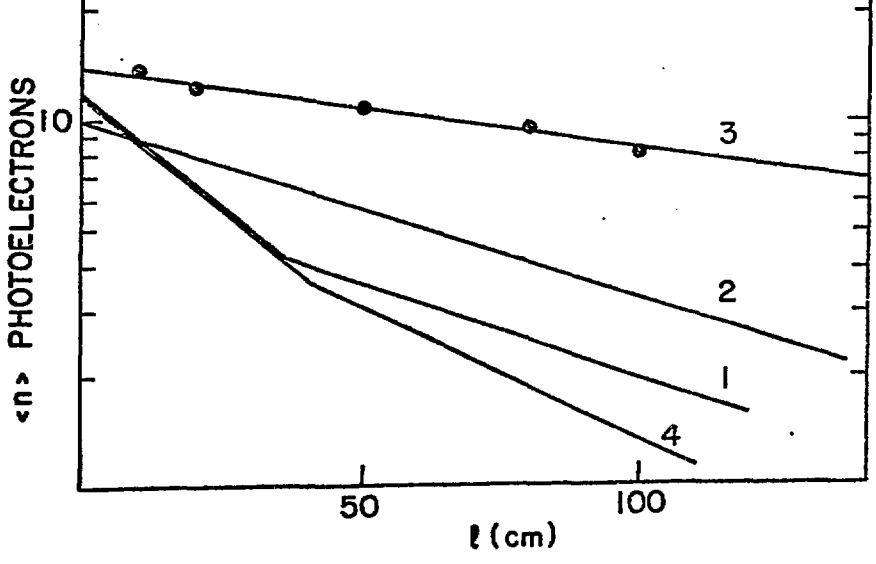

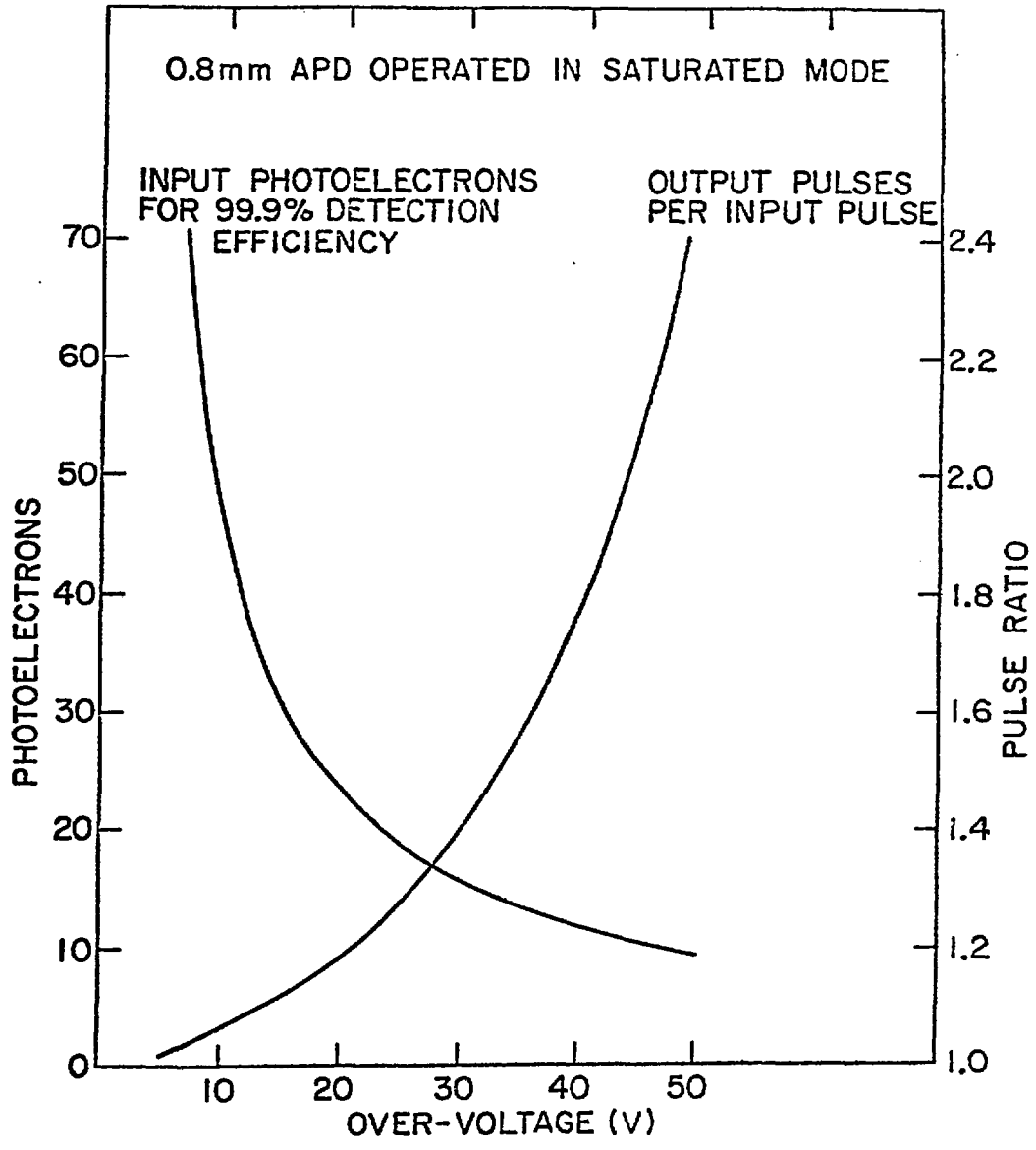
0.8mm APD OPERATED IN SATURATED MODE
INPUT PHOTOELECTRONS FOR 99.9% DETECTION EFFICIENCY
OUTPUT PULSES PER INPUT PULSE
PHOTOELECTRONS
PULSE RATIO
OVER-VOLTAGE (V)
0
10
20
30
40
50
60
70
1.0
1.2
1.4
1.6
1.8
2.0
2.2
2.4
10
20
30
40
50

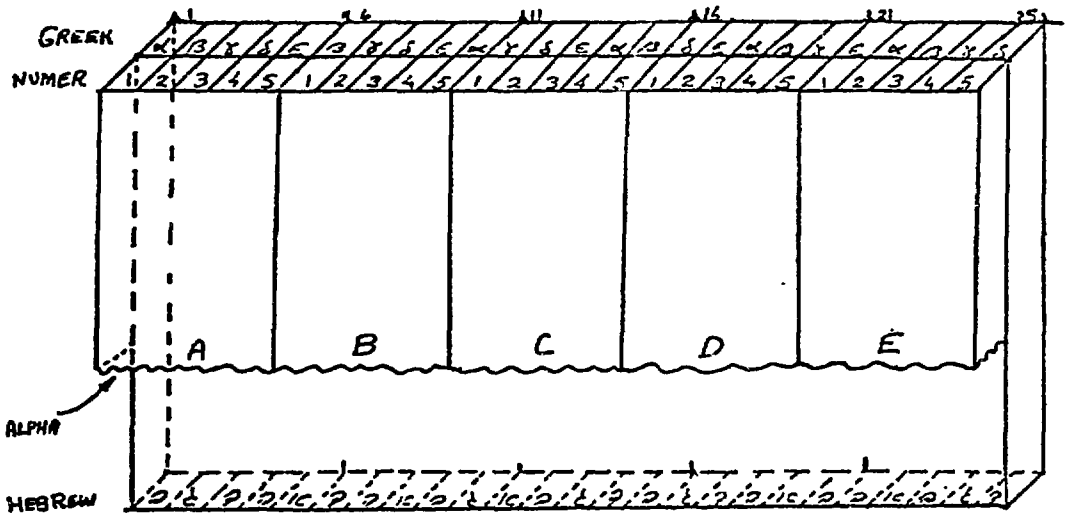

Elements hit: 2, 9, 20 = A2B4D5

Signal = ABD245βεγ ב ק

Hyp	Required	Signal	Absent	Extra
2, 9, 20	A2B4D5	β ε γ ב ק	0	0
2, 10, 19	A2B5D4	β א ב כ	2	3
4, 7, 20	A4B2D5	ד γ ק ק	2	3
4, 10, 17	A4B5D2	ד א ε ק ב ר	4	3
5, 7, 19	A5B2D4	ε γ β כ ק	2	2
5, 9, 17	A5B4D2	ε	כ ק ר	2	3

Figure 5. Optical Encoding and Ambiguity Resolution.